

# A NONLINEAR LOWPASS FILTER THAT ELIMINATES PEAK ATTENUATION

James McNames\*

Portland State University  
Biomedical Signal Processing Laboratory  
Electrical and Computer Engineering  
Portland, OR

Brahm Goldstein

Oregon Health and Science University  
Complex Systems Laboratory  
Department of Pediatrics  
Portland, OR

## ABSTRACT

Linear-phase lowpass filters are often used as a preprocessing step in signal processing applications to eliminate high frequency components of noise that do not overlap with the signal spectrum. Signals with sharp peaks confound this type of noise reduction because sharp peaks have a broad spectrum and are significantly attenuated by lowpass filters. This paper describes a simple method that restores the signal peaks to their full amplitude by adding a filtered estimate of the peak residuals to the original lowpass filter output. Examples are given of the nonlinear filter applied to a Poisson process, an electrocardiogram, and an extracellular microelectrode recording of neuron action potentials.

## 1. INTRODUCTION

Many interesting signals can be modeled as non-overlapping all-or-none events with additive noise. Examples of biomedical signals with this property include the QRS complex in electrocardiograms (ECG), electroencephalograms (EEG), and action potentials in neuronal recordings. Lowpass filters are often applied in the early stages of processing these signals to reduce noise. If the events contain sharp peaks, the user must choose a cutoff frequency that optimizes the tradeoff between elimination of the noise and attenuation of the sharp peaks. Fig. 1 shows an example of this problem when a lowpass filter is applied to an electrocardiogram signal. In this example the filter does a good job at eliminating the high frequency noise between the two beats, but the filter also significantly attenuates the peaks of each beat. This paper describes a method of restoring these peaks to their full amplitude by adding a scaled and filtered estimate of the peak residuals.

## 2. PEAK DISCRIMINATION

The nonlinear filtering algorithm described in this paper requires a method of detecting the peaks. For many well-studied signals such as the electrocardiogram, electroencephalogram, and neuronal recordings, a number of peak discriminators have been proposed in the literature [1–6]. In the absence of a signal-specific peak discriminator, one can use the simple method described in this section.

Fig. 2 shows a block diagram of our method of peak discrimination. Once the signal is filtered, the residual is found by taking the difference between the original signal and the filtered signal,  $\tilde{x}(n) \equiv x(n) - y(n)$ . This residual is then filtered with the same

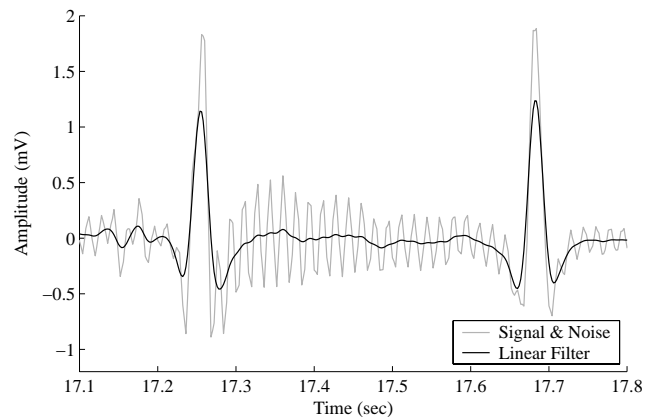


**Fig. 1.** Example of peak attenuation caused by linear-phase lowpass filters in an electrocardiogram signal. The filter zero-phase delay and a cutoff frequency of 20 Hz. Although much of the noise between the beats is eliminated by the filter, it also caused significant attenuation of the peaks of each QRS complex.

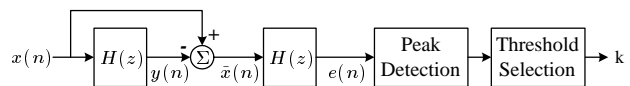
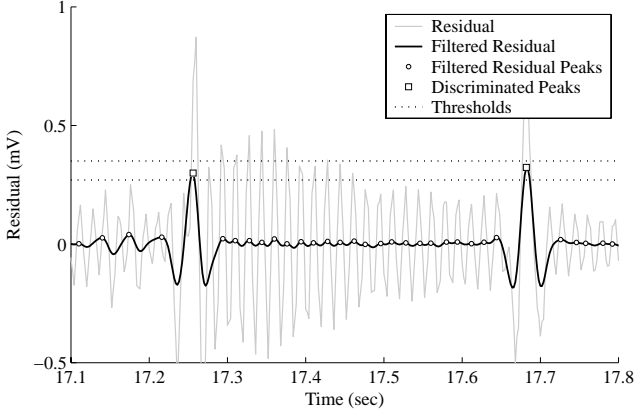


**Fig. 2.** Block diagram of a simple peak discrimination method. The thresholds for peaks are chosen from the distribution of peaks in the filtered residual,  $e(n)$ .  $H(z)$  represents the linear zero-phase lowpass filter.

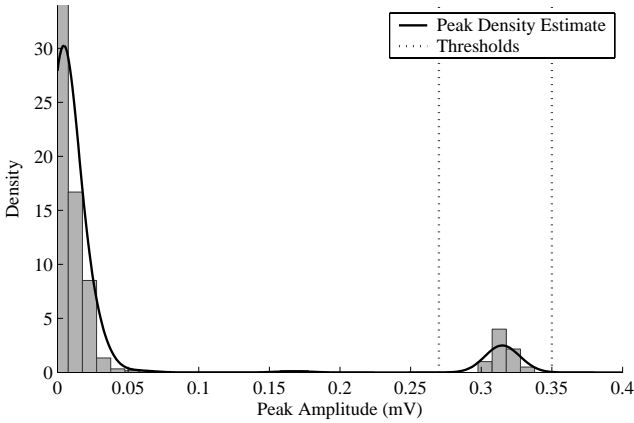
lowpass filter to produce the filtered residual  $e(n)$ . A histogram and plot of the estimated density is used to help the user choose a lower and upper threshold for peaks in the filtered residual. This algorithm was designed to find peaks in the filtered residual  $e(n)$  rather than the filter output  $y(n)$  because the filtered residual peaks distinguish between sharp peaks that are significantly attenuated and broad peaks that may have minimal attenuation.

Fig. 3 shows an example of the residual, the filtered residual, and the discriminated peaks. Fig. 4 shows the histogram and estimated density of the peaks from a 20 s electrocardiogram segment. The density was estimated using a kernel smoother [7]. The thresholds, shown by the dotted vertical lines, were selected manually to isolate the bump corresponding to peaks in the filtered residual.

\*Email: mcnames@pdx.edu. Web: ece.pdx.edu/~mcnames.



**Fig. 3.** Example of the residual  $\tilde{x}(n)$  and the filtered residual  $e(n)$  of the same electrocardiogram segment shown in Fig. 1. The dotted horizontal lines show the user-specified thresholds that demarcate the discriminated peaks.



**Fig. 4.** Example of the estimated density of peaks in the filtered residual of a 20 s electrocardiogram signal. The dotted vertical lines show the user-specified thresholds.

### 3. ALGORITHM DESCRIPTION

Fig. 5 shows a block diagram of the new nonlinear lowpass filter algorithm. The cutoff frequency of this filter is defined as the cutoff frequency of the linear lowpass filter used in this algorithm.

This algorithm requires that the low-frequency drift in the signal  $x(n)$  be removed and that the peaks of interest have a similar morphology. The algorithm described in this section requires a noncausal, lowpass filter with zero phase shift. The generalization to causal, linear-phase filters is straightforward and can be achieved by adding appropriate delays in the feed-forward paths of Fig. 5. The algorithm has been designed so that it could be implemented in an online system.

1. **Peak Range Detection.** As the peak discriminator locates the maximum of each peak, this stage finds the beginning and ending of each peak. The range of points that compose each peak is defined as the smallest consecutive group of non-negative points in the filtered residual  $e(n)$  that encompass the peak. Fig. 6 illustrates the range of two peaks

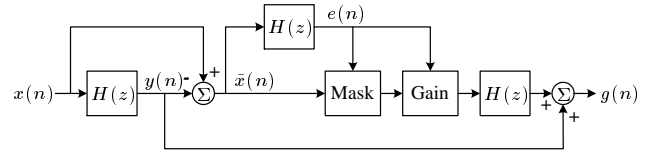


**Fig. 5.** Block diagram of the nonlinear lowpass filter algorithm designed to restore peaks.  $H(z)$  represents the linear zero-phase lowpass filter. The masking and gain stages require a peak discriminator (not shown).

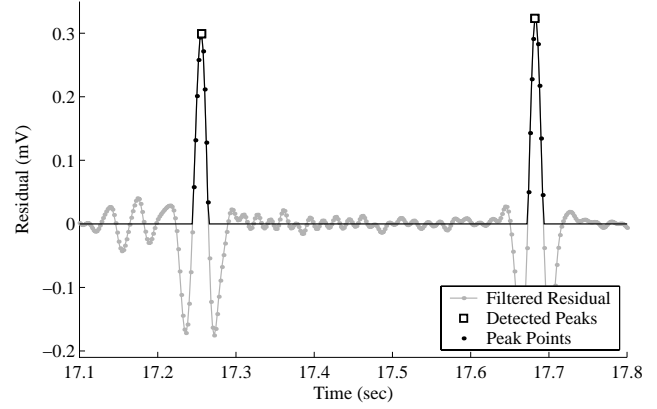


**Fig. 6.** Example of how the range of each peak is found from the filtered residual  $e(n)$  for an electrocardiogram signal.

in an electrocardiogram residual signal.

2. **Residual Masking.** Next, the residual  $\tilde{x}$  is masked and all of the points in the residual outside the range of each peak are set equal to zero. Fig. 7 shows an example of this masking stage.
3. **Gain Estimation.** Filtering the masked residual in the last stage of this algorithm attenuates the residual peaks. Thus, adding these filtered peaks would not fully restore the peaks in the signal. This stage recursively estimates the gain necessary to compensate for the attenuation caused by the residual filter in Stage 5 of this algorithm. For each peak detected, the compensating gain is approximately equal to the ratio of the peak in the residual to the peak in filtered residual,  $\tilde{x}(n)/e(n)$ . To reduce the variability of this estimate, a first-order recursive lowpass filter is used to calculate the compensating gain  $a$ ,

$$a \Leftarrow \gamma a + (1 - \gamma) \frac{\tilde{x}(n)}{e(n)}, \quad (1)$$

where  $\Leftarrow$  is the assignment operator, and  $\gamma$  is a user-specified parameter that controls the cutoff frequency of the gain filter. For all of the results reported in this paper  $\gamma = 0.9$  and the gain filter is initialized with a value of one.

4. **Amplification.** Each masked residual is then amplified by the current gain estimate,  $a$ .
5. **Residual Filtering.** The masked and amplified residual is then filtered with the linear lowpass filter  $H(z)$ . An example of this restored residual is shown in Fig. 7.

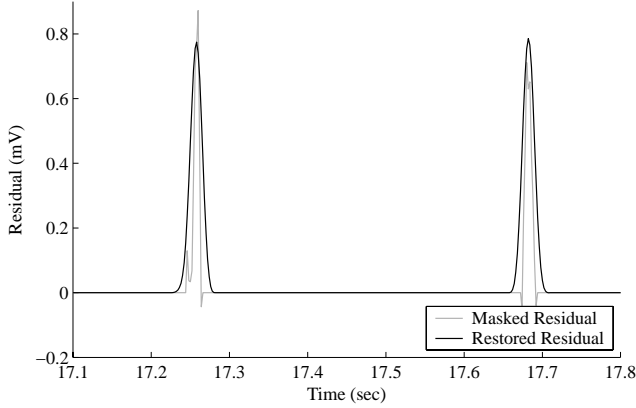


**Fig. 7.** Example of the masked residual and the restored residual for an electrocardiogram signal. Note that the restored residual has a peak amplitude that is similar to the masked residual, but the peak is broader and smoother due to the lowpass filtering of the residual.

6. **Residual Addition.** Finally, the filtered residual is added to the output of the linear lowpass filter,  $y(n)$  to produce the final output,  $g(n)$ .

#### 4. PERFORMANCE

To assess the performance of the new algorithm, synthetic signals with 100,000 points were created from a Poisson process with an average inter-arrival time of 250 samples. The peaks were Gaussian with a standard deviation of 3.9 samples. This signal was scaled to have zero mean and unit variance. White Gaussian noise was added with various amplitudes to create a series of signals with a range of signal-to-noise ratios (SNR). Both filters were applied to each noisy signal and compared to the original signal without noise. Both filters had a fixed cutoff frequency of 0.05 cycles per sample (0.31 radians/sample).

Two measures of accuracy were used to compare the linear and nonlinear filters to the signal without noise. First, the mean squared error (MSE) across the entire signal was calculated for each SNR. Since the signal had zero mean and unit variance, a MSE of one implies the estimate is no better than an estimate of zero for the entire signal. The second error measure was the MSE at the peak times.

Fig. 8 shows an example of the linear and nonlinear lowpass filters applied to this synthetic signal with an SNR of 0.75. Fig. 9 shows the two measures of error versus the SNR. This figure indicates that the nonlinear filter performs significantly worse when the noise power is greater than the signal power (SNR < 0.75). This is largely due to the inability to accurately discriminate peaks. The nonlinear filter performs modestly better than the linear filter when the SNR > 1. The nonlinear filter was substantially better than the lowpass filter at estimating the peak amplitudes as long as the SNR was large enough (SNR > 0.75) to accurately discriminate the peaks.

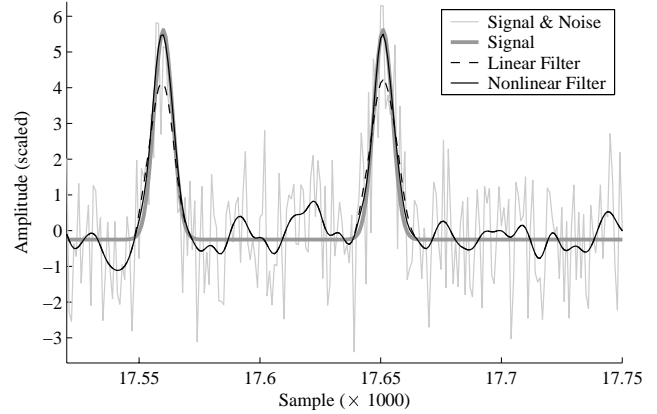


**Fig. 8.** Example of the linear and nonlinear lowpass filters applied to a Poisson process with sharp Gaussian peaks and white Gaussian noise. The signal-to-noise ratio (SNR) for this example was 0.75 and the cutoff frequency of both filters was 0.05 cycles per sample.

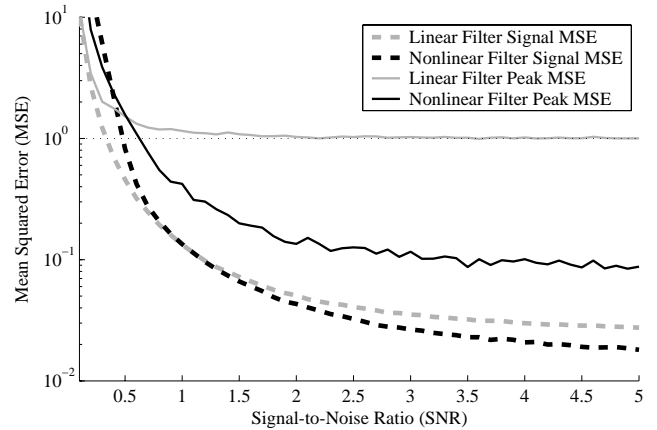


**Fig. 9.** Mean squared error versus signal-to-noise ratio (SNR) for the synthetic signal created from a Poisson process with Gaussian peaks and white Gaussian noise.

#### 5. DISCUSSION

Figs. 10 and 11 show examples of linear and nonlinear lowpass filters applied to an electrocardiogram signal and an extracellular neuronal signal, respectively. The electrocardiogram signal was recorded from a pediatric patient in the Pediatric Intensive Care Unit at Doernbecher Children's Hospital, OHSU.

The neuronal signal is a microelectrode recording acquired during neurosurgery from the globus pallidus of a patient with Parkinson's disease [8]. This example demonstrates a generalization of the algorithm to restore both positive and negative peaks. This is achieved by repeating the first four stages of the algorithm for each negative peak detected. Since the negative peaks may have a different shape and attenuation caused by the filter, they must have a separate peak discriminator and gain coefficient. The masked and amplified residuals from positive and negative peaks are summed prior to the residual filtering in the fifth stage of the algorithm.

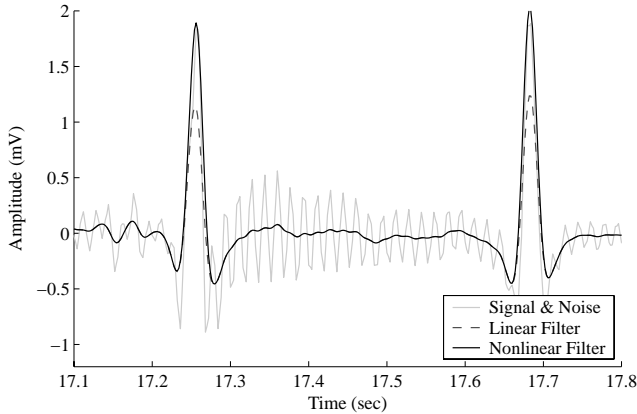


**Fig. 10.** Example of peak attenuation caused by a linear lowpass filter and the restored peaks of the nonlinear lowpass filter. This electrocardiogram signal was filtered with a zero-phase FIR filter. The sample rate was 500 Hz and the cutoff frequency of both filters was 20 Hz. Note that both filters attenuate much of the noise between the two beats, but the QRS complex is significantly attenuated by the linear filter.

The nonlinear lowpass filtering algorithm described in this paper was designed to perform the same as a lowpass filter in regions without peaks and to compensate for the attenuation of peaks while still reducing high-frequency noise. Like linear lowpass filters, this can distort and broaden the morphology of the peak. The degree and significance of this distortion depends on the filter cutoff frequency, the linear filter design, and the application.

The requirement of a peak discriminator limits the applicability of this technique as a preprocessor. This is not a severe limitation because there is usually little harm in restoring false peaks as well as the peaks of interest. Thus the algorithm could be used as one stage in an iterative peak discrimination algorithm.

For all of the examples used in this paper, symmetric non-causal finite impulse response (FIR) filters were used with positive coefficients. These filters are equivalent to weighted moving average filters. Although these filters are poor approximations of ideal lowpass filters, they are well suited to signals with sharp peaks because they do not produce ringing. Filters that have a sharper rolloff in the frequency domain can produce significant ringing and the gain estimate calculated in the third stage of the algorithm may be inaccurate as a result.

## 6. SUMMARY

This paper introduced a simple nonlinear extension of linear-phase lowpass filters to restore attenuated signal peaks. The filter may be used to restore positive peaks, negative peaks, or both. Examples of the filter applied to an electrocardiogram and a microelectrode recording of extracellular neuronal activity were given. A MATLAB implementation of this filter is available on the web at <http://bsp.pdx.edu>.

## 7. REFERENCES

[1] Jan H. Cocatre-Zilgien and Fred Delcomyn, "A slope-based approach to spike discrimination in digitized data," *Journal of*

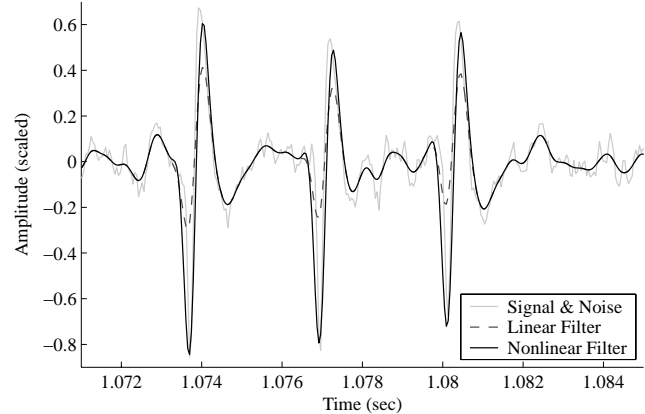


**Fig. 11.** Example of a linear lowpass filter and the nonlinear lowpass filter applied to a microelectrode recording from the globus pallidus of a patient with Parkinson's disease. For this example, the nonlinear filter was configured to restore both positive and negative peaks. The sample rate was 22 kHz and the cutoff frequency of both filters was 1000 Hz.

*Neuroscience Methods*, vol. 33, pp. 241–249, 1990.

- [2] Gary M. Friesen, Thomas C. Jannett, Manal Afify Jadallah, Stanford L. Yates, Stephen R. Quint, and H. Troy Nagle, "A comparison of the noise sensitivity of nine QRS detection algorithms," *IEEE Transactions of Biomedical Engineering*, vol. 37, no. 1, pp. 85–98, Jan. 1990.
- [3] Hagai Bergman and Mahlon R. DeLong, "A personal computer-based spike detector and sorter: Implementation and evaluation," *Journal of Neuroscience Methods*, vol. 41, pp. 187–197, 1992.
- [4] Cuiwei Li, Chongxun Zheng, and Changfeng Tai, "Detection of ECG characteristic points using wavelet transforms," *IEEE Transactions of Biomedical Engineering*, vol. 42, no. 1, pp. 21–28, Jan. 1995.
- [5] Michael S. Lewicki, "A review of methods for spike sorting: The detection and classification of neural action potentials," *Network: Computation in Neural Systems*, vol. 9, pp. R53–R78, 1998.
- [6] G. Calvagno, M. Ermani, R. Rinaldo, and F. Sartoretto, "A multiresolution approach to spike detection in EEG," in *IEEE International Conference on Acoustics, Speech and Signal Processing*, June 2000, pp. 3582–3585.
- [7] M. P. Wand and M. C. Jones, *Kernel Smoothing*, Number 60 in Monographs on Statistics and Applied Probability. Chapman & Hall, 1995.
- [8] Philip Starr, Jerrold L. Vitek, and Roy A.E. Bakay, "Ablative surgery and deep brain stimulation for Parkinson's disease," *Neurosurgery*, vol. 43, no. 5, pp. 989–1015, 1998.